ISSN 0020-4412, Instruments and Experimental Techniques, 2012, Vol. 55, No. 4, pp. 423–428. © Pleiades Publishing, Ltd., 2012.
Original Russian Text © D.Yu. Akimov, I.S. Aleksandrov, V.A. Belov, A.I. Bolozdynya, A.A. Burenkov, Yu. V. Efremenko, M.A. Kirsanov, A.S. Kobyakin, A.G. Kovalenko, A.M. Konovalov, A.V. Kumpan, V.N. Stekhanov, 2012, published in Pribory i Tekhnika Eksperimenta, 2012, No. 4, pp. 6–13.

NUCLEAR EXPERIMENTAL TECHNIQUE

Measurement of Single-Electron Noise in a Liquid-Xenon Emission Detector

D. Yu. Akimov[a], I. S. Aleksandrov[a], V. A. Belov[a], A. I. Bolozdynya[b], A. A. Burenkov[a], Yu. V. Efremenko[b,c], M. A. Kirsanov[b], A. S. Kobyakin[a], A. G. Kovalenko[a], A. M. Konovalov[a], A. V. Kumpan[b], and V. N. Stekhanov[a]

[a] *SSC RF Institute of Theoretical and Experimental Physics, ul. Bol'shaya Cheremushkinskaya 25, Moscow, 117218 Russia*
[b] *National Research Nuclear University MEPhI, Kashirskoe sh. 31, Moscow, 115409 Russia*
e-mail: avkumpan@gmail.com
[c] *The University of Tennessee, 1331 Circle Park Drive, Knoxville, Tennessee, 37996 USA*

Received November 30, 2011

Abstract—A technique for studying single-electron noise in emission detectors that are intended for detection of rare processes with small energy releases is developed. Examples of possible applications are experiments for search of dark matter in the Universe and detection of reactor antineutrinos via coherent neutrino scattering at heavy xenon nuclei. We present the first results of studying the nature of single-electron noise in a liquid-xenon emission detector and consider possible ways to suppress it.

DOI: 10.1134/S002044121204001X

1. INTRODUCTION

The emission method for detecting tracks of ionizing particles was proposed at the Department of Experimental Physics of Moscow Engineering Physics Institute forty years ago [1]. It was implemented in several instruments, including the emission streamer chamber [2]. Subsequently, it was shown that film-free (electron) emission detectors (EDs) that operate in the wall-less mode are promising in studies of rare processes with small energy deposition [3, 4].

Since that time, such detectors have been widely used in experiments on the search for cold dark matter in the Universe in the form of weakly interacting massive particles (WIMPs). The best up-to-date limits on the cross section of WIMP–nucleon interaction for WIMPs with a mass around ~100 GeV/c^2 were obtained with ZEPLIN-III and XENON100 liquid-xenon EDs [5, 6]. The XENON100 detector contains 170 kg of liquid xenon and is presently being exposed at the Gran Sasso underground laboratory (Italy) [6]. The new LUX detector with 350 kg of xenon is being prepared for the experiment at the underground laboratory in the Homestake mine (USA) [7].

In addition to the search for dark matter in the form of WIMPs, EDs are considered to be a promising tool for detection and study of coherent scattering of reactor antineutrinos. Neutrino coherent scattering of heavy atoms produce recoil nuclei with kinetic energies in the kiloelectronvolt range [8].

2. PROCESSES LIMITING THE SENSITIVITY OF EMISSION DETECTORS

The principle of particle detection in two-phase noble-gas EDs is as follows. Ionization electrons that are produced by radiation in the condensed phase of the working medium in a detector are extracted with an applied electric field to the gas phase, where electrons drift in a quite high electric field and generate luminescence of the gas, called electroluminescence. The latter is remarkable because it yields a high-intensity light signal (several hundreds of photons per each ionization electron) that is proportional to the number of electrons or ionization yield.

In addition, in liquid noble gases, the ionization is accompanied by excitation of atoms that leads to generation of a prompt scintillation flash. Thus, an ionizing particle is detected with two signals—a fast scintillation signal and an electroluminescence signal, which is delayed by the electron drift time to the surface of the condensed phase. This method allows one not only to measure the spatial position of the primary-interaction point but also to efficiently reject background signals that are associated with the radioactivity of surrounding materials [9].

During R&D on detectors for dark matter search, several groups of researchers observed that signals in the form of single-photoelectron noise frequently appeared after intense scintillation and electroluminescence light flashes [10–13]. In [12], it was shown that single-photoelectron signals are clustered in groups with a total duration typical of electroluminescence signals. Analysis of the distributions of cluster over their areas has shown that these have characteris-

Electron properties of liquid and solid nonpolar dielectrics that are most frequently used in emission detectors [9]

Dielectrics	T, K	ε	μ_0, cm^2/V/s	V_0, eV	E_c, kV/cm	E_0, kV/cm	t_e, μs (E, kV/cm)
Emitters of cold electrons							
Liquid Ar	84	1.51	475	–0.21	0.2		700 (0.1)
Emitters of hot electrons							
Liquid Ar	84	1.51	475	–0.21	0.2	0.25	<0.1 (>0.3)
Solid Ar	83		1000	+0.3 (6 K)		0.1	<0.1 (>0.1)
Liquid Xe	161	1.93	2200	–0.61	0.05	1.75	<0.1 (>1.8)
Solid Xe	161		4500	–0.46 (40 K)		1.25	<0.1 (>1.3)

Note: μ_0 is the electron mobility in the zero-field approximation; V_0 is the potential energy of the electron ground state; E_c is the critical field in which electron heating is initiated; E_0 is the field corresponding to the emission threshold; and t_e is the emission time.

tic peaks corresponding to the signal from one electron. For the setup described in [13] and used in this study, a single electron produces on average 15 photoelectrons in seven photomultipliers (PMTs).

The presence of such kind of noise associated with spontaneous (i.e., uncorrelated with any signals) single-electron electroluminescence signals is a factor limiting the sensitivity of EDs to weak-ionizing particles. Signals of such a small value (on the order of a few electrons) are expected in experiments on the detection of coherent scattering of neutrinos off nuclei [8, 14].

Single-electron signals may arise as a result of the following processes:

(1) spontaneous emission of electrons accumulated under the surface barrier at the interface between different phases;

(2) photoemission by electroluminescence light of electrons from negative ions accumulated under the interface;

(3) photoemission of electrons from the cathode illuminated by very intense electroluminescence the gaseous phase (e.g., after passing of a cosmic muon through the detector).

In this study, we investigated the conditions for the appearance of single-electron noise and possible ways to suppress it.

3. FEATURES OF ELECTRON TRANSPORT THROUGH THE INTERFACE BETWEEN THE PHASES

Let us consider the specific features of the electron transport through the interface between the xenon liquid and gas phases that exist in thermodynamic equilibrium.

Because the dielectric permittivities of different phases of nonpolar dielectrics are different, electric-charge carriers experience the action of the potential A of image polarization nature (this potential is created by the electric field of the charge itself), which acts against the charge transfer from the denser medium to the medium with the lower density:

$$A_{1,2} = -e(\varepsilon_1 - \varepsilon_2)/[4\varepsilon_{1,2}(z + \xi z/|z|)(\varepsilon_1 + \varepsilon_2)], \quad (1)$$

where ε is the relative permittivity; indices 1 and 2 refer to the condensed and equilibrium gas phases, respectively; z is the coordinate along the normal to the interface between the phases (positive values correspond to the gas phase); and ξ is the cut-off parameter having an order of magnitude of the transition layer between the phases (approximately several nanometers).

The potential of charge image depends on the temperature and approaches zero at temperatures that are close to the critical one.

The total potential energy of electrons near the interface can be described in terms of a one-dimensional potential that depends only on the coordinate z, which is normal to the interface between the phases and directed out of the condensed phase:

$$\begin{aligned} V_1(z) &= V_0 - eE_1 z + eA_1, \quad z < 0; \\ V_2(z) &= -eE_2 z + eA_2, \quad z > 0. \end{aligned} \quad (2)$$

Here, E_1 is an electric field that is used to extract electrons from the condensed phase, the ground state of an electron is characterized by the potential V_0 (see the table), and the image potential is taken from (1).

In terms of this one-dimensional approximation, an electron that approaches the surface can penetrate into it "outright," if the projection of its momentum p_z along the z axis exceeds the threshold $p_0 \approx (2m_e|V_0|)^{1/2}$, as it is shown for the upper electron trajectory in Fig. 1. If $p_z < p_0$, the electron will be most likely reflected from the potential barrier back to the condensed phase, where it will be thermalized after several collisions with atoms in the medium (see the lower electron trajectory in Fig. 1). The electrons localized under the surface as a result of such a process can nevertheless escape from the condensed dielectric owing to thermal electron emission process, although this process may require a significant time.

The charge carriers that are moving towards the surface under the external electric field $\vec{E}$, which is applied normally to the interface so that $\varepsilon_1 E_1 = \varepsilon_2 E_2$, can be concentrated in the denser phase near the interface at the depth z_0 that corresponds to the minimum of potential $V_1(z)$:

$$z_0 = -\left[\frac{e}{4E_1}\,\frac{\varepsilon_1 - \varepsilon_2}{\varepsilon_1(\varepsilon_1 + \varepsilon_2)}\right]^{1/2}. \quad (3)$$

After thermalization, these carriers occupy the space with linear dimensions of an order of

$$l = 3kT/(2eE_1). \quad (4)$$

Under certain favorable conditions, charge carriers may be extracted from the condensed phase through the free surface to the neighboring gaseous phase. The emission of charge carriers can be characterized by the emission time t_e that is required for penetration through the surface barrier by an electron with an average velocity v_z, which is directed normally to the interface:

$$t_e = l/v_z. \quad (5)$$

The average velocity of charge carriers that penetrate through the surface barrier can be calculated as

$$v_z = P \int\limits_{p_z > p_0} \alpha\beta \frac{p_z}{m} f(\vec{p})\, d\vec{p}, \quad (6)$$

where P is the probability of being in the quasi-free state for a charge carrier ($P = 1$ for liquid xenon); α is the coefficient of potential-barrier penetrability that depends on the profile of the potential near the barrier and the charge-carrier wave function; β is the probability to avoid backscattering; p_0 is the threshold momentum magnitude in the direction towards the interface between the phases; and $f(\vec{p})$ is the momentum distribution function for carriers. The potential-barrier penetrability α for massive ions is extremely low. Electrons with small effective masses in some nonpolar dielectrics, such as heavy condensed noble gases including liquid xenon, can efficiently penetrate through the surface potential barrier.

If the characteristic emission time t_e significantly exceeds the relaxation time of the momentum distribution function $f(\vec{p})$, the emission can be considered as a slow and virtually stationary process. Then, the number of charge carriers accumulated under the interface due to the influence of the external field can be written as

$$N(t) = N_0 \exp(-t/t_e), \quad (7)$$

where N_0 is the initial number of electrons that arrived at the interface.

If the lifetime of quasi-free electrons (the main object of our interest) is limited by the time t_c till the moment of their trapping by an electronegative impurity, expression (7) must be corrected as:

$$N(t) = N_0 \exp(-t/t_e - t/t_c). \quad (8)$$

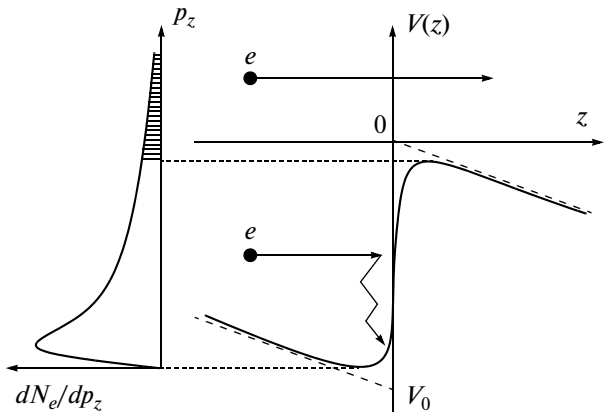

Fig. 1. Emission of hot electrons from a nonpolar dielectric with a negative energy of the ground state of quasi-free electrons V_0 into the rarefied phase ($z > 0$).

The total number of electrons emitted within the time t could be calculated by integration of the emission rate $dN(t)/dt$ obtained from (7):

$$N_e(t) = N_0 t_c (t_e + t_c)^{-1} \{1 - \exp[-(t_e + t_c)t/(t_e t_c)]\}. \quad (9)$$

The electron emission is often characterized by the probability or emission coefficient, which, using formula (8), can be defined as

$$K_e = N_e(\infty)/N_0 = (1 + t_e/t_c)^{-1}. \quad (10)$$

4. ELECTRON EMISSION FROM LIQUID XENON

The effective emission (with an emission coefficient $K_e \sim 1$) of quasi-free electrons was observed from condensed noble gases, methane, and some liquid saturated hydrocarbons that are characterized by the high electron mobility. In general, the electron emission from nonpolar dielectrics looks like a threshold process. The value of the observed field threshold E_0 is strongly correlated with the value of the ground electron state V_0 in the condensed phase; namely, the negative V_0 values correspond to large E_0 values (see the table).

In liquid argon, the height of the potential barrier at the interface between the phases is comparable with the kinetic energy of quasi-free electrons that are in thermodynamic equilibrium with the medium: $V_0 \sim kT$. In this case, there is a sufficient number of electrons in the high-energy "tail" of the momentum distribution function ($p_z > p_0$, Fig. 1) that can be emitted at the expense of the thermal energy of the medium. However, the penetration through the potential barrier may take much time depending on the electric-field strength that influences the barrier width. Indeed, it was shown in [9] that the characteristic emission time t_e of thermal electrons from liquid isooctane and liquid argon is inversely proportional to the applied "extract-

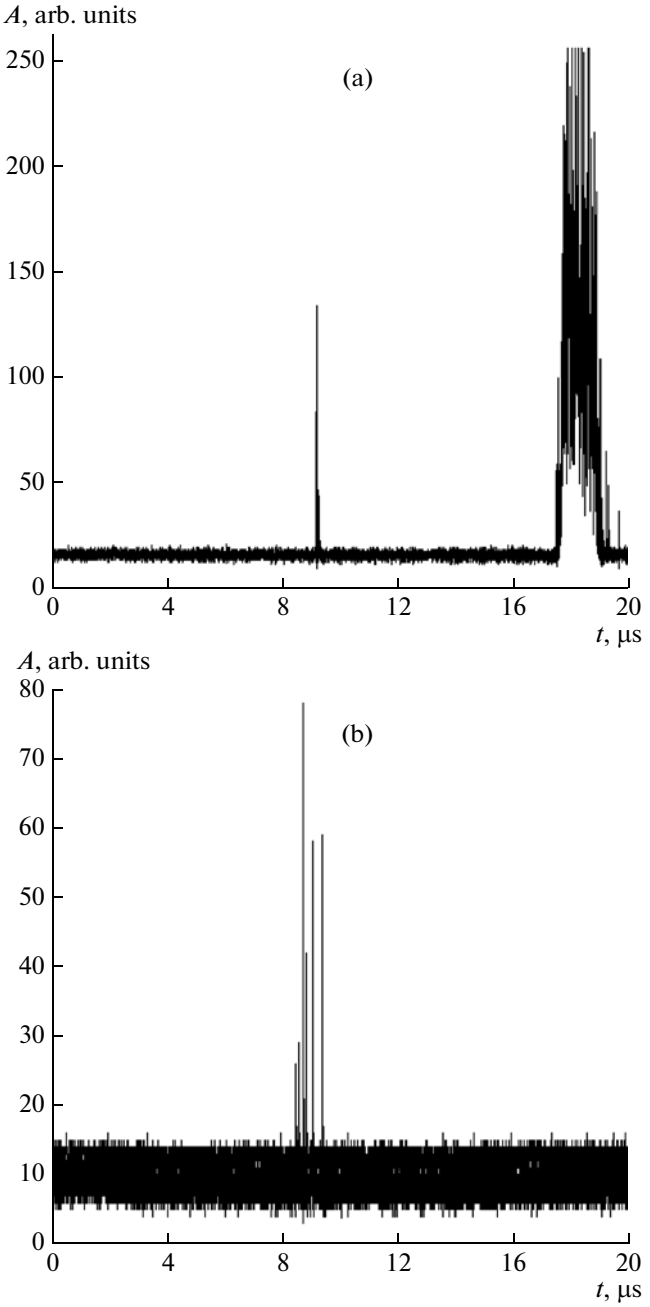

Fig. 2. Oscillograms of (a) a typical signal from a γ photon with an energy of ~100 keV and (b) a single-electron electroluminescence signal.

ing" electric strength changing from 10^{-3}–10^{-6} s, as follows from formulas (4) and (5).

In condensed xenon, the potential barrier of the interface is so high ($|V_0| >> kT$) that, at the purification levels that are achieved today, the lifetime t_c of quasi-free electrons is much shorter than the emission time t_e. Therefore, no thermal electron emission from these media was observed. On the other hand, in the condensed xenon, it is rather easy to reach such an electric-field strength E_c in which the average kinetic energy of drifting electrons exceeds the thermal energy to such a degree that even electroluminescence of the condensed phase can be produced. Under such conditions, a significant fraction of electrons may acquire a momentum $p_z > p_0$ and be emitted without a delay after arriving at the interface.

In order to empirically describe the effective emission of hot electrons, the value of the emission "threshold" electric field E_0 is commonly used (see the table). Electrons that were not emitted are quickly (within ~1 ps) thermalized because they have reached the interface and cannot continue to drift. After that, they can be emitted only as thermal electrons or will be trapped by electronegative impurities and transform into negative ions, which accumulate under the interface. The appearance of single electrons in the gas is theoretically possible as a result of emission of electrons from negative ions under intensive electroluminescence caused by a particle with high ionization losses.

In any case, the accumulation of nonemitted electrons near the interface can cause the emission of electrons that are not directly related to the particle detection; i.e., these electrons will generate parasitic noise during detection of signals from weakly ionizing particles.

5. THE TECHNIQUE FOR MEASURING SINGLE-ELECTRON NOISE

Single-electron noise was studied using the experimental setup that was described in [13]. This detector is a cylindrical stainless-steel vessel with a plane–parallel electrode system filled with liquid xenon at a temperature of 172 K. The cathode is made as a grid of 0.1-mm-diameter wires with a 1-mm pitch. To increase the light collection, the anode was made as a disk a specular reflective surface. The distances from the cathode to the surface of the liquid phase and from the liquid-xenon surface to the anode are 22 and 5 mm, respectively. The diameter of the working region of the detector is 105 mm. An array of seven ФЭУ-181 PMTs is placed in the liquid xenon under the wire cathode and is used for detection of scintillation in the liquid phase and electroluminescence in the gas phase.

A typical signal from the ED for a γ ray with an energy of ~100 keV is shown in Fig. 2a. This signal consists of two parts. The leading pulse is caused by the scintillation in the liquid phase, and the trailing one corresponds to electroluminescence in the gas phase. The electroluminescence pulse is delayed relative to the scintillation signal by the drift time of electrons moving from the interaction point of the detected particle to the liquid-phase surface.

A single-electron electroluminescence signal in this detector is a cluster of single-photoelectron pulses

from different PMTs with an overall duration of ~1 μs (Fig. 2b). This time corresponds to the time of electron drift in the gas phase. The total number of single-photoelectron signals in the cluster depends on the electric-field strength in the gas phase, the size of the gas gap, the light-collection conditions, and the quantum efficiency of the PMTs. In the described detector design, we detected on average 15 photoelectrons per single photoelectrons.

We selected only the events that were not followed by an electroluminescence flash within a time interval (inhibit time Δt_{veto}) several times longer than the electron drift time across the liquid-xenon layer $\Delta t_{veto} > t_{dr1}$. This was done to exclude the events associated with the electron photoemission from the cathode and from the negative ions accumulated under the liquid-gas xenon interface. In order to exclude signals from any real particles, we also required to exclude a scintillation signal during Δt_{veto}.

The rate of appearance of single-electron electroluminescence signals f_{1e} was measured at a selected inhibit time Δt_{veto} as a function of the applied electric field, the detector count rate under the action of an external γ-ray source, and the angle between the liquid–gas interface and the plane–parallel electrode system of the detector.

6. EXPERIMENTAL RESULTS

The performed study with the ED has shown that the intense electroluminescence in the gas gap, for example, cosmic muons, causes the appearance of additional electroluminescence signals that are delayed by the drift time of electrons from the cathode to the interface between the phases ("echo" effect). Introduction of the inhibit time for recording electroluminescence signals, which is a multiple of several drift times of electrons through the layer of liquid xenon, $\Delta t_{veto} > 3t_{dr1}$, substantially reduces the probability of such events. Therefore, recording of events during $3t_{dr1}$ after an intense electroluminescence flash was prohibited. Inhibit was also placed on recording of any events with scintillation signals that precede an event within a time interval $3t_{dr1}$.

After such selections, we mainly recorded events caused by spontaneous emission of electrons accumulated under the surface of liquid xenon as a result of irradiation with natural radiation. We observed that under such conditions, the rate of appearance of single-electron electroluminescence signals f_{1e} depends on the strength of the electric field E_1 (Fig. 3). In the first approximation, this agrees with expressions (4) and (5).

In fact, $f_{1e} \sim 1/t_e$, and as follows from (4) and (5), $f_{1e} \sim v_z E_1$. Because v_z must increase with an increase in the electric-field strength, the count rate of single-electron signals must increase faster than the linear function U (the anode–cathode voltage). Thus, the experimental data presented in Fig. 3 qualitatively correspond to the model described in Section 3.

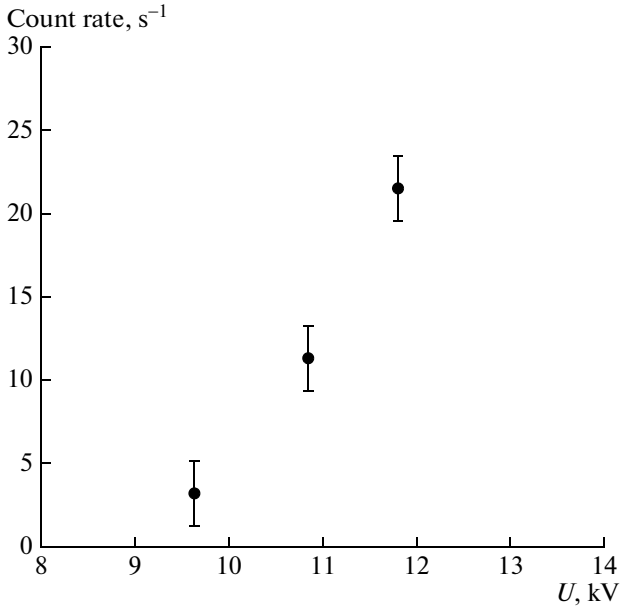

Fig. 3. The count rate of single-electron signals of the liquid xenon emission detector as a function of the potential difference between the anode and cathode.

When we placed a radioactive source next to the detector, we observed both an increase in the rate of single-electron signals and an increase in the detector count rate, which corresponds to this model as well.

The observed influence of the detector tilt with respect to the horizon was another confirmation of the considered model of the origin of single-electron noise, which is not related to intense electroluminescence. Initially, the plane–parallel two-electrode system of the detector was installed horizontally. We measured the single-electron rate in the detector when it was slightly tilted in one direction and then by the same angle in the opposite direction. The voltage between the anode and cathode was 11 kV. Figure 4 shows the results of measuring the single-electron rate as a function of the detector tilt angle.

As can be seen in Fig. 4, the rate of single electrons f_{1e} decreased by a factor of ~2 at a detector tilt angle of ~0.3°. The possible interpretation of this result is that the component of the electric field tangential to the surface sweeps out electrons accumulated under the surface in liquid xenon.

7. CONCLUSION

The following conclusions can be made on the basis of the results studying single-electron noise in the liquid-xenon emission chamber:

(1) Single-electron noise is mostly associated with the spontaneous emission of electrons that accumulate under the interface between the phases.

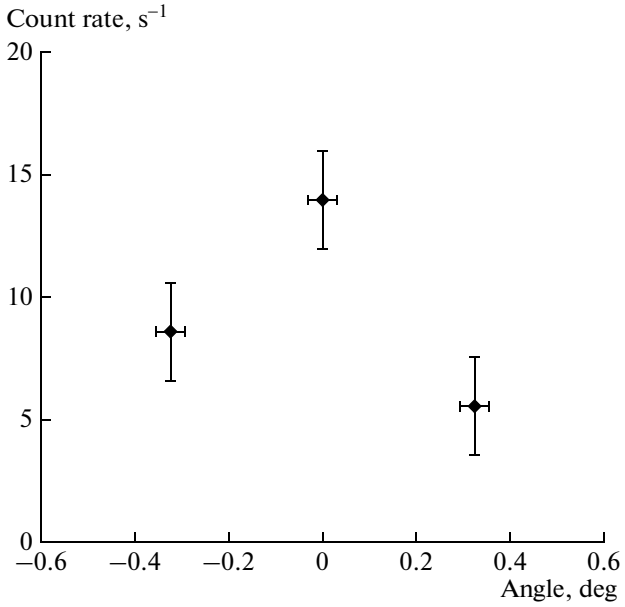

Fig. 4. The count rate of single-electron signals as a function of the angle between the liquid surface and the horizon for 11-kV potential difference between the anode and cathode.

(2) A weak tangential electric field (on the order of several tens of volts per centimeter) causes a substantial decrease in the intensity of such noise and can be used for improving the signal-to-noise ratio in detectors for particles with a low ionizing power.

Currently, the authors are setting up a problem of a more detailed study of the revealed effects.

ACKNOWLEDGMENTS

This study was supported by the Russian Foundation for Basic Research (project no. 11-02-00668-a), the State Contract no. P881 as a part of the Federal Targeted Program "Scientific and Scientific–Pedagogical Staff of Innovation Russia, 2009–2013," and a grant of the Government of the Russian Federation (resolution no. 220 according to contract no. 1.G34.31.0049). This research is a part of the RED collaboration program for design of a new-generation neutrino detector.

REFERENCES

1. Dolgoshein, B.A., Lebedenko, V.N., and Rodionov, B.U., *Pis'ma Zh. Eksp. Teor. Fiz.*, 1970, vol. 11, p. 351.
2. Bolozdynya, A.I., Egorov, O.K., Miroshnichenko, V.P., et al., in *Elementarnye chastitsy i kosmicheskie luchi. Vyp. 5* (Elementary Particles and Cosmic Rays), Moscow: Atomizdat, 1980, p. 65.
3. Bolozdynya, A., Egorov, V., Rodionov, B., et al., *IEEE Trans. Nucl. Sci.*, 1995, vol. 42, p. 565.
4. Bolozdynya, A., *Nucl. Instrum. Meth. A*, 1999, vol. 422, p. 314.
5. Akimov, D.Yu., Araujo, H.M., Barnes, E.J., et al., E-print: arXiv:1110.4769v1 [astro-ph.CO] 2011.
6. Aprile, E., Arisaka, K., Arneodo, F., et al., *Phys. Rev. Lett.*, 2011, vol. 107, p. 131302.
7. Fiorucci, S., Akerib, D.S., Bedikian, S., et al., E-print: arXiv:0912.0482v1 [astro-ph.CO] 2009.
8. Akimov, D., Bondar, A., Burenkov, A., and Buzulutskov, A., *JINST*, 2009, vol. 4, p. 06010.
9. Bolozdynya, A., *Emission Detectors*, Singapore: World Sci., 2010.
10. Akimov, D.Yu., Bewick, A., Danilov, M.V., et al., *Phys. Atom. Nucl.*, 2003, vol. 66, no. 3, p. 497.
11. Yamashita, M., Dark Matter Search Experiment with Double Phase Xe Detector, *Phil. Degr. Thesis*, Tokyo: Waseda University, 2003.
12. Edwards B., Araujo H.M., Chepel V. et al., *Astropart. Phys.*, 2008, vol. 30, p. 54; E-print: arXiv:0708.0768v1 [physics.ins-det] 2007.
13. Burenkov A.A., Akimov D.Yu., Grishkin Yu.L., et al., *Phys. Atom. Nucl.*, 2009, vol. 72, no. 4, p. 653.
14. Hagmann, C. and Bernstein, A., *IEEE Trans. Nucl. Sci.*, 2004, vol. 51, p. 2151.